Retinoblastoma gene mutations detected by whole exome sequencing of Merkel cell carcinoma

Patrick J Cimino[1], Diane H Robirds[1], Sheryl R Tripp[2], John D Pfeifer[1], Haley J Abel[3] and Eric J Duncavage[1]

[1]*Department of Pathology and Immunology, Division of Anatomic and Molecular Pathology, Washington University School of Medicine, Saint Louis, MO, USA;* [2]*ARUP Laboratories, Salt Lake City, UT, USA and* [3]*Division of Statistical Genomics, Washington University School of Medicine, Saint Louis, MO, USA*

Merkel cell carcinoma is a highly aggressive cutaneous neuroendocrine tumor that has been associated with Merkel cell polyomavirus in up to 80% of cases. Merkel cell polyomavirus is believed to influence pathogenesis, at least in part, through expression of the large T antigen, which includes a retinoblastoma protein-binding domain. However, there appears to be significant clinical and morphological overlap between polyomavirus-positive and polyomavirus-negative Merkel cell carcinoma cases. Although much of the recent focus of Merkel cell carcinoma pathogenesis has been on polyomavirus, the pathogenesis of polyomavirus-negative cases is still poorly understood. We hypothesized that there are underlying human somatic mutations that unify Merkel cell carcinoma pathogenesis across polyomavirus status, and to investigate we performed whole exome sequencing on five polyomavirus-positive cases and three polyomavirus-negative cases. We found that there were no significant differences in the overall number of single-nucleotide variations, copy number variations, insertion/deletions, and chromosomal rearrangements when comparing polyomavirus-positive to polyomavirus-negative cases. However, we did find that the retinoblastoma pathway genes harbored a high number of mutations in Merkel cell carcinoma. Furthermore, the retinoblastoma gene (*RB1*) was found to have nonsense truncating protein mutations in all three polyomavirus-negative cases; no such mutations were found in the polyomavirus-positive cases. In all eight cases, the retinoblastoma pathway dysregulation was confirmed by immunohistochemistry. Although polyomavirus-positive Merkel cell carcinoma is believed to undergo retinoblastoma dysregulation through viral large T antigen expression, our findings demonstrate that somatic mutations in polyomavirus-negative Merkel cell carcinoma lead to retinoblastoma dysregulation through an alternative pathway. This novel finding suggests that the retinoblastoma pathway dysregulation leads to an overlapping Merkel cell carcinoma phenotype and that oncogenesis occurs through either a polyomavirus-dependent (viral large T antigen expression) or polyomavirus-independent (host somatic mutation) mechanism.
Modern Pathology (2014) **27,** 1073–1087; doi:10.1038/modpathol.2013.235; published online 10 January 2014

Keywords: Merkel cell carcinoma; retinoblastoma; whole exome sequencing; polyomavirus

Merkel cell carcinoma is a rare neuroendocrine tumor of the skin with an aggressive clinical course and an increased prevalence in the elderly and immunosuppressed.[1] The incidence of Merkel cell carcinoma has increased in the last several decades, and the United States has an estimated incidence rate of 0.32 per 100 000 persons per year.[2] Merkel cell carcinoma has a predilection for sun exposed areas, most often occurring in the head and neck region.[3] There is an overall 5-year survival rate of 40%, with stage being a significant prognosticator.[3,4] Merkel cell polyomavirus was discovered in Merkel cell carcinoma and found to be clonally integrated in ~80% of cases.[5–7] Merkel cell polyomavirus has a high seroprevalence in the general population and asymptomatic infection begins in childhood.[8–11] As one of the steps in the proposed mechanism for Merkel cell carcinoma oncogenesis, polyomavirus

Correspondence: Dr EJ Duncavage, MD, Department of Pathology and Immunology, Division of Anatomic and Molecular Pathology, Washington University School of Medicine, 660 Euclid Avenue, Box 8118, Saint Louis, MO 63110-1093, USA.
E-mail: EDuncavage@path.wustl.edu
Received 5 July 2013; revised 25 October 2013; accepted 1 November 2013; published online 10 January 2014

must integrate into the human genome.[12] Viral integration sites occur throughout the human genome without apparent specificity.[13,14] Emerging data implicate maintenance and expression of the polyomavirus large T antigen in cell cycle dysregulation and the pathogenesis of viral transformation leading to Merkel cell carcinoma.[12,15–21] Although the molecular role of Merkel cell polyomavirus is quickly evolving, the overall biology of Merkel cell carcinoma is poorly understood. Moreover, the presence of polyomavirus alone is not sufficient for carcinogenesis, namely in those Merkel cell carcinoma cases considered as polyomavirus-negative.

With established subpopulations of polyomavirus-positive and polyomavirus-negative Merkel cell carcinoma, there has been interest in defining what similarities and differences exist between these groups, especially with regard to clinical outcomes and histology. To date, there is somewhat controversial data regarding the clinical outcomes between polyomavirus status Merkel cell carcinoma subpopulations. An early Finnish study of 114 Merkel cell carcinoma samples by Sihtu *et al*[7] showed that polyomavirus-positive cases had a significantly higher (threefold) 5-year overall survival when compared with polyomavirus-negative cases. In a smaller United States study (23 cases) by Bhatia *et al*,[22] median survival was approximately fourfold longer in polyomavirus-positive cases (86 months) than in polyomavirus-negative cases (20 months). In contrast, three subsequent studies by Handschel *et al*[23] (44 German cases), Schrama *et al*[24] (146 Australian and German cases), and Asioli *et al*[25] (70 Italian cases) demonstrated that 5-year overall survival is independent of Merkel cell polyomavirus status. Additionally, it does not appear that polyomavirus status influences recurrence-free survival.[24] Although there have been reported subtle, yet statistically significant, nuclear and cytoplasmic differences between polyomavirus-positive and polyomavirus-negative Merkel cell carcinoma as detected by complex morphologic analysis,[26] the two are fairly indistinguishable in routine pathological examination of Merkel cell carcinoma by light microscopy.

Despite the conflicting data regarding the outcome and Merkel cell polyomavirus status, it is clear that there is a phenotypic, morphologic, and clinical overlap between polyomavirus-positive and polyomavirus-negative cases. Although Merkel cell polyomavirus is believed to have a role in the majority of cases, a significant proportion ($\sim$20%) of Merkel cell carcinoma is polyomavirus-negative. The existence of Merkel cell polyomavirus-negative cases demonstrates that polyomavirus alone is not sufficient for the development of Merkel cell carcinoma. Thus, it is likely that the Merkel cell carcinoma phenotype develops through distinct, yet convergent, polyomavirus-dependent and polyomavirus-independent mechanisms. The molecular and cellular determinants of these convergent phenotypes have yet to be fully established. In this study, we tested the hypothesis that there are somatically acquired mutations in the human genome, which lead to overlapping morphological and clinical Merkel cell carcinoma phenotypes. We performed whole exome sequencing of polyomavirus-positive and polyomavirus-negative cases as an unbiased approach to detect recurrent somatic mutations in Merkel cell carcinoma and to investigate the possible role of known cancer pathways in Merkel cell carcinoma development.

Materials and methods

Case Selection

The use of human subject material was performed in accordance with guidelines set by the Institutional Review Board of Washington University. Eight total cases from deceased patients were selected for whole exome sequencing from previously published and characterized Merkel cell carcinoma cases for which sufficient tissue from formalin-fixed paraffin-embedded blocks was available for DNA testing and confirmatory studies.[13,27] Clinical characteristics included five patients with metastatic Merkel cell carcinoma and three patients with no reported metastases (summarized in Table 1).

Merkel Cell Polyomavirus Detection

Total genomic DNA was extracted from formalin-fixed paraffin-embedded tissue blocks as previously described.[13] To determine Merkel cell polyomavirus status, standard polymerase chain reaction was performed using previously published protocols. Briefly, thermocycler conditions were as follows: (1) 55 °C, 1 min; (2) 95 °C, 1 min; (3) 95 °C, 15 sec; (4) 55 °C, 1 min; and (5) repeat steps 3 and 4 for 35 cycles. Platinum Taq HF (Invitrogen, Grand Island, NY, USA) was used. The MCVPS1 primer set was used to detect Merkel cell polyomavirus as previously published;[5] forward sequence 5′-TCAGCGTCCCAG GCTTCAGA-3′, reverse sequence 5′-TGGTGGTCTCC TCTCTGCTACTG-3′. A similarly sized beta-globin product (110 bp) was used as an amplification control (forward sequence 5′-ACACAACTGTGTTCA CTAGC-3′; reverse sequence 5′-CAACTTCATCCACG TTCACC-3′). Cloned viral plasmid DNA (pMCV-R17a) was used as a positive control, and no template reactions and DNA from normal controls were used as negative controls. Polymerase chain reaction products were detected by agarose gel electrophoresis following ethidium bromide staining. Five of the cases had reliably detected Merkel cell polyomavirus by standard polymerase chain reaction (06, 18, 24, 27, and 39) and were considered polyomavirus-positive cases. The other

Table 1 Demographics and Merkel cell polyomavirus status

Case number	*Age at diagnosis (years)*	*Age at death (years)*	*Sex*	*Primary site of involvement*	*Site of metastases*	*Polyomavirus (copy/cell)*	*Polyomavirus-positive vs negative*
24	47	50	M	Skin, right neck	Lymph nodes, lower neck	10	+
06	78	81	M	Skin, left eyelid	—	5	+
27	81	82	F	Skin, right upper arm	—	5	+
39	78	79	M	Skin, left buttock	Lymph nodes, left groin	0.1	+
18	83	94	F	Skin, right cheek	—	0.01	+
33	51	53	F	Skin, left upper leg	Lymph nodes, left groin	0.005	−
29	70	83	M	Skin, left temple	Lymph nodes, left neck	<0.0004	−
21	66	68	M	Skin, posterior scalp	Lymph nodes, left posterior triangle	<0.0004	−

Abbreviations: F, female; M, male.

three cases (21, 29, and 33) were polyomavirus-negative.

To ensure maximal viral sensitivity, we further determined the Merkel cell polyomavirus copy number using a sensitive, previously published real-time polymerase chain reaction assay.[22,27,28] Briefly, thermocycler conditions were as follows: (1) 50 °C, 1 min; (2) 95 °C, 1 min; (3) 95 °C, 15 sec; (4) 60 °C, 1 min; and (5) repeat steps 3 and 4 for 40 cycles. Applied Biosystems (Carlsbad, CA, USA) ABI Taqman assay primers were used for the conserved Merkel cell polyomavirus small T antigen, with the following primer sequences: forward sequence 5′-GCAAAAAAACTGTCTGACGTGG-3′; reverse sequence 5′-CCACCAGTCAAAACTTTCC CA-3′; probe sequence 5′-TATCAGTGCTTTATTC TTTGGTTTGGATTTCCTCCT-3′. Cloned MCPyV (pMCV-R17a) viral plasmid was serially diluted and used as the positive control, and no template reactions were used for the negative control. The detection threshold was determined from the threshold cycle (C_t) of the most diluted positive control. The sensitivity of this assay is estimated to be ~0.0004 viral copies/cell.[27,28]

Whole Exome Sequencing

One microgram of total genomic DNA (as determined by Qubit (Life Technologies, Grand Island, NY, USA)) from each of the eight Merkel cell carcinoma cases was first fragmented to ~200–300 base pairs using a Covaris E210 instrument (Covaris Inc., Woburn, MA, USA) then end-repaired and ligated to universal Illumina sequencing adapters. Sequencing libraries were then hybridized to Agilent V4 exome capture probes as per the manufacturer's instructions (Agilent Technologies, Santa Clara, CA, USA). Captured DNA was then subjected to limited cycle polymerase chain reaction amplification (eight cycles) using primers with seven base pair sequence indexes to permit multiplex sequencing. DNA from two to three cases was then pooled in equimolar volumes and each pool was sequenced on a HighSeq2000 lane using 2 × 101 base pair paired end reads. Base calls and quality scores were generated by the included Casava software (v1.8).

Data Analysis

The resulting FASTQ files were aligned to NBCI build 37.2 of the human reference genome (hg19) using Novoalign (Novocraft, Selangor, Malaysia) with default paired-end parameters. Quality metrics were then calculated using a variety of publicly available software and sequence data were 'cleaned' to mark duplicate reads, recalibrate quality scores, and realigned around known polymorphisms using the Genome Analysis Toolkit (GATK v1.6)[29,30] (http://www.broadinstitute.org/gatk) and picard tools (http://picard.sourceforge.net). Sequence variation was identified using multiple software tools to capture the full spectrum of DNA variation; single-nucleotide polymorphisms and small (<10 base pairs) insertions and deletions (indels) were determined using samtools[31] (http://samtools.sourceforge.net) to ensure a low false-positive rate; larger indels (>10 base pairs) were identified using Pindel[32] (https://trac.nbic.nl/pindel); translocations were identified using Breakdancer[33] (http://breakdancer.sourceforge.net); and copy number variation was identified using CONTRA[34] (http://contra-cnv.sourceforge.net). Sequence variants were then annotated using the SeattleSeq annotation server (http://gvsbatch.gs.washington.edu/SeattleSeqAnnotation137/index.jsp) and only variants representing coding region changes in at least one transcript, and not present as constitutional polymorphisms in dbSNP (v130) (http://www.ncbi.nlm.nih.gov/projects/SNP), were considered for further analysis. The resulting novel coding region changes were compared with previously published somatic cancer mutations using the COSMIC database (v64)[35,36] (http://cancer.sanger.ac.uk/cancergenome/projects/cosmic). Further, to ensure that previously described somatic variants

were not inadvertently removed from the analysis by filtering known polymorphisms in dbSNP, all detected single-nucleotide variations were compared with COSMIC and manually reviewed.

As paired normal tissue was not available for analysis, we could not directly differentiate between coding region changes representing 'personal single-nucleotide polymorphisms' (rare mean allele frequency variants not present in dbSNP) and true somatic mutations. Therefore, we used mutation recurrence among all eight cases to determine which genes were most likely implicated in Merkel cell carcinoma pathogenesis. Coding region variants not present in dbSNP were compared at the gene level (any mutation in the gene) among all cases and segregated by Merkel cell polyomavirus status using custom R scripts (available upon request). High frequency recurrent single-nucleotide variations (present in >five of eight cases) were further filtered against a laboratory-generated 'blacklist' of false-positive variants resulting from sequence alignment errors particular to the Agilent V4 exome capture probes. The observed allele fractions of mutations were used to infer co-occurring mutations as has been previously described.[37]

Fluorescence *In Situ* Hybridization

Interphase fluorescence *in situ* hybridization for *RB1* was performed on formalin-fixed paraffin-embedded tissue sections cut at a thickness of 5 μm on positively charged microscope slides. The paraffin was removed from the sections with three washes of 5 min each in CitriSolve. The slides were then hydrated in two washes of absolute ethanol for 1 min each and allowed to air dry. The slides were processed through a pretreatment solution of sodium thiocyanate that had been preheated to 80 °C. After a 3 min wash in distilled water, the tissue was digested in protease solution (pepsin in 0.2N HCl) for 15 min at 37 °C, followed by another 3 min wash in distilled water. The slides were allowed to air dry after which they were dehydrated by passing through consecutive 70, 85, and 100 ethanol solutions for 1 min each. The slides were again allowed to air dry before applying prepared probe mixture. Probes used were purchased from Abbott Molecular (Des Plaines, IL, USA) and included Vysis LSI 13 (RB1) 13q14 SpectrumOrange Probe (Catalog no. 05J15-011) and Vysis 13q34 SpectrumGreen fluorescence *in situ* hybridization Probe Kit-CE (Catalog no. 05N34-020). Probes were diluted at a concentration of 1:50 in *t*DenHyb-2 hybridization buffer (Insitus Biotechnologies Inc., Albuquerque, NM, USA) and well-mixed. Next, the probe in buffer was applied to the appropriate slide to cover the tissue section and the section was coverslipped. Co-denaturation was achieved by incubating the slides at 73 °C for 5 min in a slide moat. Hybridization occurred by transferring the slides to a 37 °C slide light-shielded, humid slide moat overnight. Post hybridization, the coverslips were removed and the slides immersed in 75 °C wash solution (2XSSC/0.3%NP40) for 2 min followed by a 1 min wash in jar containing the same solution at room temperature. The slides were allowed to air dry in the dark and were then counterstained with 10 μl of DAPI II (Abbott Molecular Inc.). Slides were examined using an Olympus BX60 fluorescent microscope with appropriate filters for SpectrumOrange, SpectrumGreen, and the DAPI counterstain. The signal patterns were documented using a CoolSnap camera and Cyto Vision Imaging System.

Immunohistochemistry

Immunohistochemistry utilized formalin-fixed paraffin-embedded tissue cut at 5 μm sections and floated onto charged slides. Immunohistochemistry for the retinoblastoma protein was performed by Clarient Inc. (Aliso Viejo, CA, USA). Primary antibodies used included retinoblastoma antibody (clone G3-245; BD Biosciences San Jose, CA, USA) at 1:300 dilution for 30 min and phospho-retinoblastoma (Ser807/811) antibody (Catalog 9308; Cell Signaling Technology, Boston, MA, USA) at 1:200 dilution for 1 h. Automated staining was performed using the Bond-III Autostainer (Leica, Buffalo Grove, IL, USA) for retinoblastoma and Ventana Benchmark XT (Ventana Medical, Tucson, AZ, USA) for phospho-retinoblastoma according to the manufacturer's protocol. Pretreatment antigen retrieval strategies included Leica Bond Epitope Retrieval solution 2 (EDTA-based buffer, pH 9.0) for retinoblastoma and a protein citrate buffer (pH 6.0) for phospho-retinoblastoma at 100 °C. Breast cancer specimens were used as positive staining controls.

Statistics

Comparisons made between groups were performed using the GraphPad Prism software (La Jolla, CA, USA) and the *R* statistics package (*R*, version 2.15.1, *R* Project for Statistical Computing, http://www.r-project.org/). *P*-values were determined by the use of the two-tailed unpaired *t*-test. Plots were created in *R*.

Results

Demographics and Sequence Metrics

Eight cases of Merkel cell carcinoma that have been previously reported were included in this study (representative Merkel cell carcinoma histology shown in Figure 1).[13,27] Demographic information is summarized in Table 1. Five cases were Merkel cell polyomavirus-positive and the other three were polyomavirus-negative as determined by using the MCVPS1 primer set and agarose gel detection. The

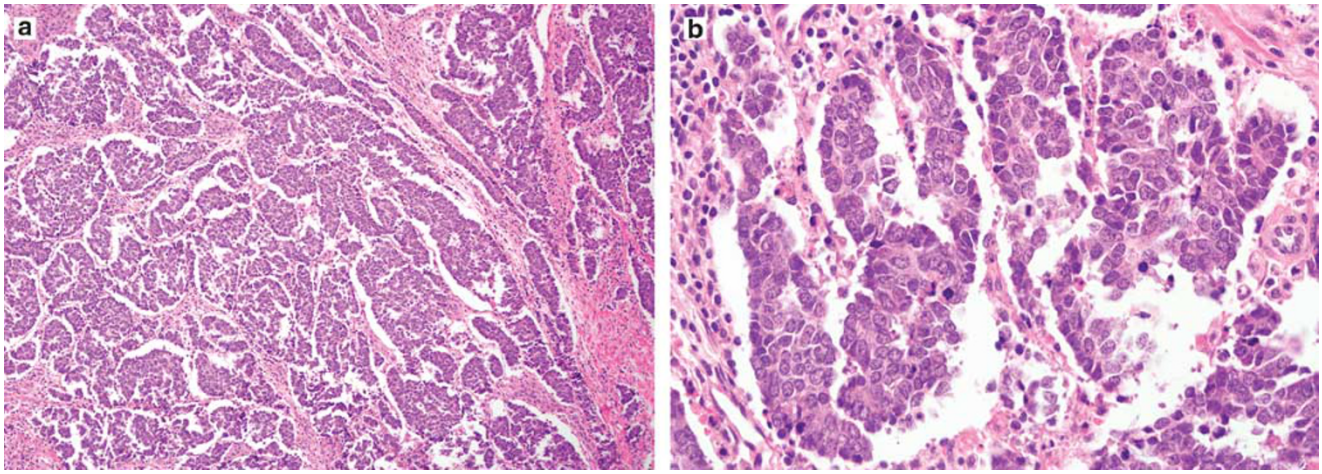

Figure 1 Representative hematoxylin and eosin-stained sections of Merkel cell carcinoma. The tumor comprises sheets and nests of infiltrative high-grade neuroendocrine carcinoma. (**a**) Low power (×100 original magnification). (**b**) High power (×400 original magnification).

Table 2 Total number and types of mutations identified by whole exome sequencing

Merkel cell polyomavirus status	*Case*	*Total single-nucleotide variations*	*Novel non-polymorphism single-nucleotide variations*	*Non-polymorphism single-nucleotide variations (nonsynonymous)*	*Total copy number variations*	*Total small indels*	*Total large indels*
Positive	06	41 188	1470	461	245	413	4
	18	43 244	4237	1570	74	363	14
	24	41 109	1409	416	876	412	6
	27	41 515	1364	411	341	382	3
	39	40 691	1236	363	143	410	39
	Average	41 549	1943	978	336	326	13
Negative	21	43 782	4188	1519	240	421	3
	29	42 192	6350	2248	184	403	365
	33	40 426	2714	925	45	393	12
	Average	42 133	4417	1815	156	329	127
P-value		0.5500	0.0632	0.694	0.3919	0.5350	0.2424

P-value determined by comparing mean values between polyomavirus status groups using the two-tailed Mann–Whitney *U* statistics. Small indels are ≤15 nucleotides and large indels are in the range of 15–1000 nucleotides in length. Copy number variations involve nucleotides greater than 1000 nucleotides.

average age at diagnosis between the polyomavirus-positive cases (73 years, ±15 years) and the polyomavirus-negative cases (62 years, ±10 years) was not significantly different ($P=0.2143$). Similarly, the length of time from diagnosis to death between polyomavirus-positive cases (4 years, ±4 years) and the polyomavirus-negative cases (6 years, ±6 years) was not significantly different ($P=0.4821$). All eight cases had a primary site located within the skin and five of eight cases showed metastases to regional lymph nodes. All three of the polyomavirus-negative cases had metastatic disease, whereas only two of the five polyomavirus-positive cases had metastases. Although a small number of cases, this is consistent with some of the controversial literature reporting a more aggressive clinical course related to polyomavirus-negative cases.[7,22,38]

Whole human exome sequencing was performed on each of the eight Merkel cell carcinoma cases using formalin-fixed paraffin-embedded tissue. The average number of reads generated per case was 130 477 404 (26 GBases). On average, 94.1% of the exome for each case had at least 25× coverage. The spectrum of mutations identified include single-nucleotide variations, copy number variations, indels (insertion/deletions), and structural variations. The total number of mutations identified, as well as the type, for each case is summarized in Table 2. Each case generated an average of 41 768 single-nucleotide variation calls, of which 989 represented novel (not in dbSNP) nonsynonymous variants. There was no significant difference in the total number of variants or novel nonsynonymous variants between polyomavirus-positive and polyomavirus-negative groups ($P=0.5500$ and

$P = 0.0632$, respectively). Small indels (as called by samtools) averaged 400 per case and showed no significant difference between polyomavirus-positive and polyomavirus-negative groups ($P = 0.5350$). Larger indels (as called by Pindel) averaged 56 per case and showed no significant difference between polyomavirus-positive and polyomavirus-negative groups ($P = 0.2424$). Similarly, copy number variations (as called by CONTRA) averaged 269 per case and showed no significant difference between polyomavirus-positive and polyomavirus-negative groups ($P = 0.3919$).

Identification of Recurrent Mutation

As paired normal samples were not sequenced along with the Merkel cell carcinoma samples, we could not differentiate between non-pathogenic 'personal single-nucleotide polymorphisms' (low mean allele frequency variants specific to an individual and not present in dbSNP) and true somatically acquired variants. Therefore, we looked for recurrent mutations among the eight Merkel cell carcinoma cases to determine genes critical to pathogenesis. Recurrence was assessed at the gene level (ie, the presence or absence of mutations in *TP53*). Recurrent mutations are summarized in Table 3. There were eight highly recurrent nonsynonymous, non-dbSNP gene variants, present in all eight cases. None of these occurred in known cancer-related genes and the same variant for each gene was observed in each case; all were flagged as 'blacklisted' variants representing sequence capture artifact, and these variants were not further analyzed, but are included in the Table 3 for completeness. Analysis of highly recurrent gene variants by Merkel cell polyomavirus status showed that no variants were specific to polyomavirus-positive Merkel cell carcinoma, whereas several genes were associated with polyomavirus-negative Merkel cell carcinoma, including the conical tumor suppressor *RB1*. All three polyomavirus-negative cases showed truncating, nonsense *RB1* mutations including chr13:g.48916767G>A (p.W99*, AF = 0.93), (chr13:g.48923137G>A, p.W195*, AF = 0.77), and chr13:g.49027222C>T (p.Q597*, AF = 0.86) located in exons 3, 6, and 18, respectively. All of these nonsense mutations were predicted to be deleterious by PolyPhen and one (p.W195*) has been previously described in breast cancer (COSMIC ID: COSS1659943).[39] To assess the significance of these findings, we compared the rate of truncating, nonsense *RB1* mutations previously reported as somatic variants in all cancer types using the COSMIC database (181 of 12 584 cases) to our data. Assuming a rate of truncating mutation in RB1 of 0.014 for both virus-positive and -negative cases of Merkel cell carcinoma, and considering all possible 2×2 tables with row sums fixed to 5 and 3 (the numbers of polyomavirus-positive and -negative cases), we obtain a highly significant *P*-value of 5.6×10^{-6} for the finding of nonsense *RB1* mutations in all three polyomavirus-negative cases, but none of the five polyomavirus-positive cases.

Table 3 Recurrence analysis of genes with nonsynonymous single-nucleotide variations

Present in all Merkel cell carcinoma cases	*Present exclusively in all polyomavirus-positive cases*	*Present exclusively in all polyomavirus-negative cases*
UGT2B15[a]	*None*	*DCAF4L1*
C1orf163[a]		*MAP3K6*
KLF14[a]		*CCDC129*
KIAA1267[a]		*BBS9*
LGI4[a]		*VCAN*
KCNC3[a]		*COL29A1*
AMDHD2[a]		*STARD9*
PRSS3[a]		*CD163L1*
		GCKR
		RB1
		COL22A1
		ODZ2
		LPPR2
		ASXL3

[a]These variants were flagged as 'blacklisted variants' and most likely represent sequence capture artifact.

Identification of RB1 and RB1 Pathway Mutations

On the basis of the finding of truncating *RB1* nonsense mutations in three of three polyomavirus-negative Merkel cell carcinoma cases, we sought to determine whether retinoblastoma-related pathway genes were mutated in polyomavirus-positive cases. Further, although the initial recurrence analysis focused only on single base pair variants, we subsequently analyzed a full range of DNA variation including indels, copy number variations, and translocations, to determine whether retinoblastoma pathway mutations were included in a broader class of mutations. Retinoblastoma pathway mutations are summarized in Table 4. All eight Merkel cell carcinoma cases showed sequence changes predicted to affect at least one of the 14 retinoblastoma pathway genes. The retinoblastoma gene (*RB1*) itself, was disrupted in five of the eight cases (including the three previously described nonsense mutations, one case with a frame-shift deletion, and one case with RB1 copy loss). The range of *RB1* mutations are summarized in Table 5. Strikingly, all three polyomavirus-negative cases had truncating single-nucleotide variant nonsense mutations, which were located in three separate locations of *RB1*; all mutations were present with a high variant allele fraction. None of the polyomavirus-positive cases had a nonsense *RB1* mutation. Two cases, one polyomavirus-positive and one polyomavirus-negative case, each had a large *RB1* deletion, and one polyomavirus-positive case had a small deletion involving *RB1*.

Table 4 Summary of the genetic mutations associated with the retinoblastoma pathway in Merkel cell carcinoma.

Retinoblastoma pathway genes	Case Number							
	24	06	27	39	18	33	29	21
ABL1								■
CCNA1					■			
CCND3					■			
CDC25A			■					
CDK2AP1				▒				
CDKN2A								■
MYC					■			■
MYCBP2		■					■	■
***RB1**			▒		▒	■	■	▒
RBBP6		▒					▒	■
RBBP7	▒	▒		▒				
RBBP8							■	
RBL1	▒				■	■		
RBL2	▒				■		■	
Polyomavirus (viral copies/cell)	10	5	5	0.1	0.01	0.005	<0.0004	<0.0004

■ Non-polymorphism single-nucleotide variation.
▒ Copy number variation.
▒ Non-polymorphism single-nucleotide variation and copy number variation.
▒ Indel.

Validation of RB1 pathway mutations

Following the discovery phase of mutations in Merkel cell carcinoma, the DNA and protein-level validation of the changes in *RB1* observed in whole exome sequencing was performed. First, the *RB1* copy number loss detected in two Merkel cell carcinoma cases by whole exome sequencing was confirmed by fluorescence *in situ* hybridization (Figure 2). Second, to determine whether mutations detected in the *RB1* gene resulted in a corresponding change in retinoblastoma protein expression, we performed immunohistochemistry for the retinoblastoma protein. Retinoblastoma protein showed absent immunoreactivity in each of the five cases with a *RB1* mutation discovered by whole exome sequencing (Figure 3); however, the three cases without *RB1* mutations by sequencing, showed strong and diffuse nuclear reactivity for the retinoblastoma protein. These results support a one to one relationship with *RB1* genetic mutations and corresponding absence of protein. To further explore the retinoblastoma pathway in Merkel cell carcinoma, immunohistochemistry for phosphorylated-retinoblastoma protein was performed. Under normal regulatory circumstances in actively cycling tumor cells, retinoblastoma protein is phosphorylated, leading to its inactivation as a tumor suppressor, S-phase entry, and cell division. Therefore, in the three Merkel cell

Table 5 Specific mutations found in the *RB1* gene of Merkel cell carcinoma

Case	*Mutation type*	*(Chr13) Position; nucleotide change*	*Amino-acid change*
18	Deletion	Chr13:49039143 to chr13:49039441	Deletion of 741–809
27	Copy number variation	48877913 to 49047550	Copy loss
33	Nonsense single-nucleotide variation	48916767; G→A	TRP→stop (99/928)
	Missense single-nucleotide variation	48916768; G→A	GLY→ARG (100/928)
21	Nonsense single-nucleotide variation	48923137; G→A	TRP→stop (195/928)
	Copy number variation	48877913 to 48878116	Copy loss
29	Nonsense single-nucleotide variation	49027222; C→T	GLN→stop (597/928)

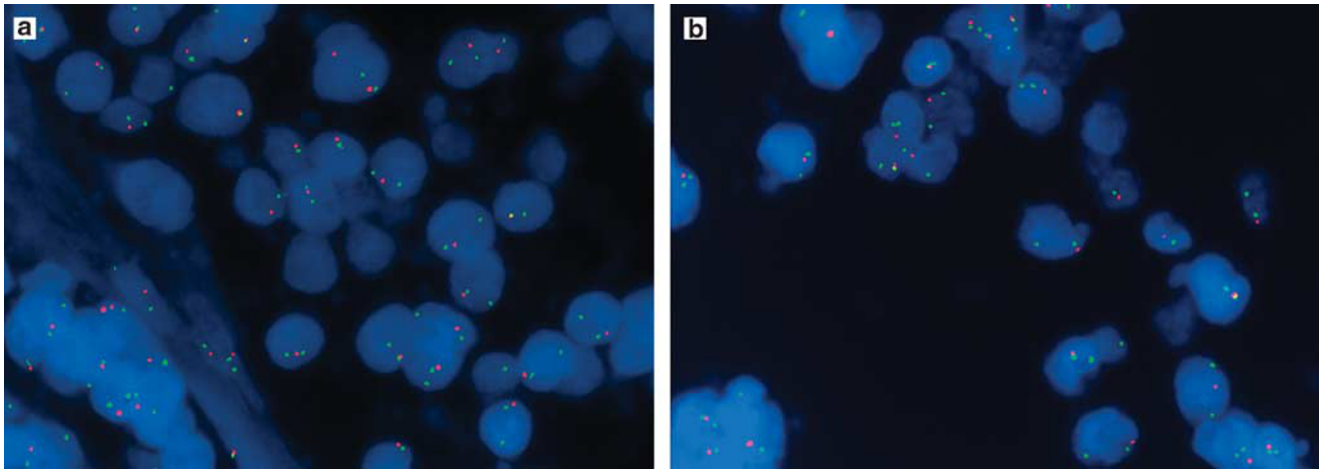

Figure 2 Fluorescence *in situ* hybridization confirms loss of *RB1* in the only two cases of Merkel cell carcinoma as discovered by whole exome sequencing. (**a**) One case is Merkel cell polyomavirus-negative (case 21). (**b**) The other case is polyomavirus-positive (case 27). Normal *RB1* copy number was observed in the other cases (not shown). Red = *RB1*; green = 13q14.

carcinoma cases with detectable retinoblastoma protein expression (Figure 3), phosphorylation of retinoblastoma protein is expected, given an intact retinoblastoma signaling pathway. However, in all eight cases, there was similar, minimal detectable phosphorylated-retinoblastoma protein, consistent with retinoblastoma dysregulation (Figure 4).

Comparison of Variant Allele Fractions

To determine whether other gene variants were part of the same founder clone containing *RB1* nonsense mutations, arising either before or at the time of the *RB1* mutation, we examined the variant allele fraction of single-nucleotide variations as has been previously described.[37] We first examined the allele fraction of single-nucleotide variations present in dbSNP (representing constitutional variants) to non-dbSNP variants (representing 'personal' constitutional variants and true somatically acquired mutations). As expected, although single-nucleotide variations present in dbSNP had allele fractions of 50 or 100% consistent with hetero- or homozygous constitutional

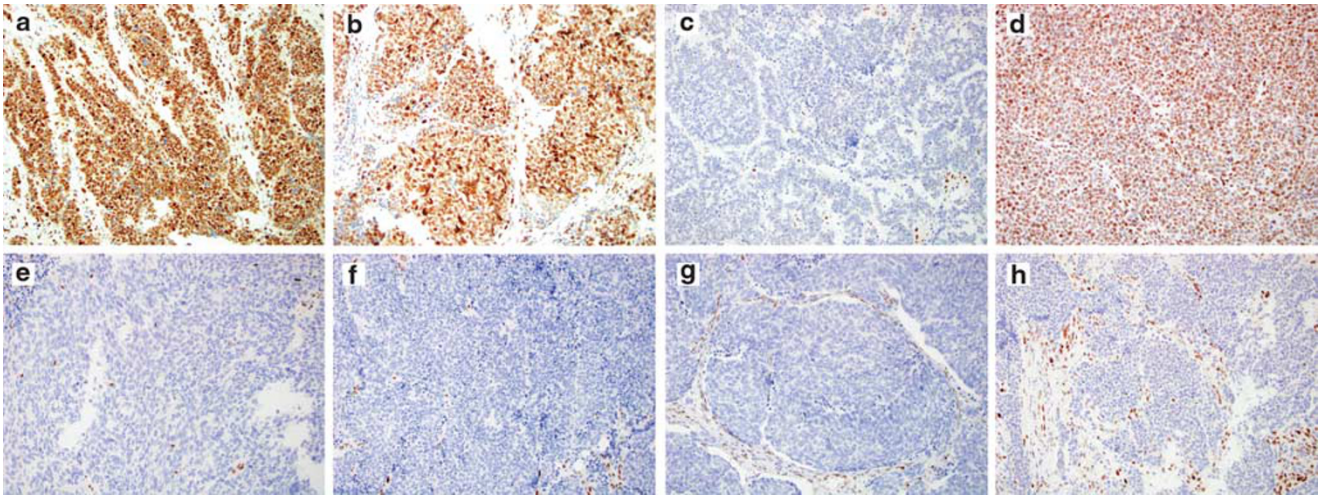

Figure 3 Retinoblastoma protein immunoreactivity is absent in all Merkel cell carcinoma cases with a genetic mutation; and reactivity is present in all cases without a detected mutation. (**a**) Case 24—retinoblastoma-positive (no genetic mutation). (**b**) Case 06—retinoblastoma-positive (no genetic mutation). (**c**) Case 27—retinoblastoma-negative (*RB1* copy number loss). (**d**) Case 39—retinoblastoma-positive (no genetic mutation). (**e**) Case 18—retinoblastoma-negative (deletion). (**f**) Case 33—retinoblastoma-negative (nonsense truncating mutation). (**g**) Case 29—retinoblastoma-negative (nonsense truncating mutation). (**h**) Case 21—retinoblastoma-negative (nonsense truncating mutation and *RB1* copy number loss). Internal positive controls for retinoblastoma are seen in stromal and lymph node lymphocytes. All images were taken at $\times 200$ original magnification.

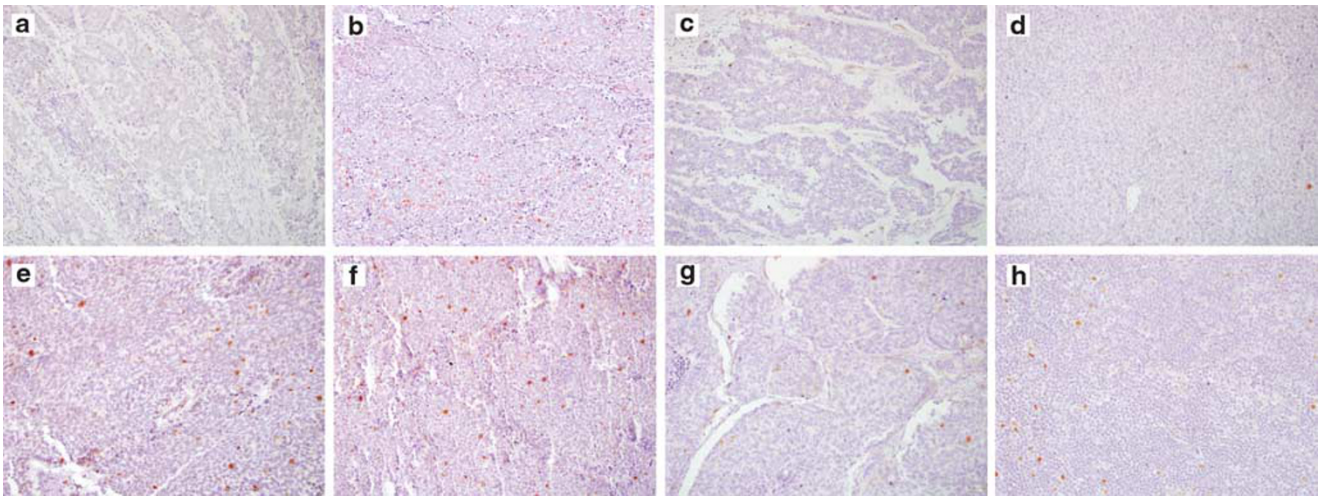

Figure 4 Phosphorylated-retinoblastoma protein immunoreactivity is absent in all Merkel cell carcinoma cases, including those with pan-retinoblastoma staining. (**a**) Case 24, (**b**) Case 06, (**c**) Case 27, (**d**) Case 39, (**e**) Case 18, (**f**) Case 33, (**g**) Case 29, and (**h**) Case 21. Internal positive controls for phosphorylated-retinoblastoma are seen in few stromal and lymph node lymphocytes. All images were taken at $\times 200$ original magnification.

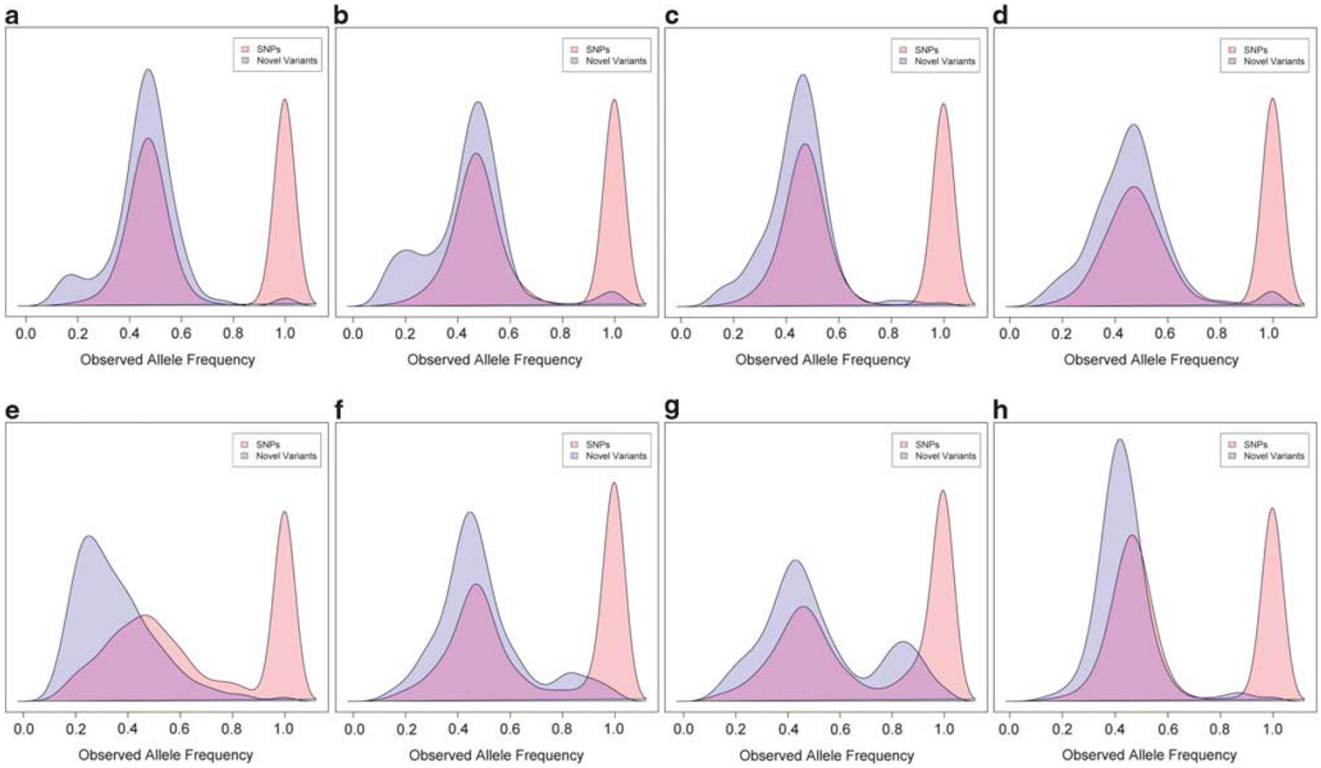

Figure 5 Variant allele fractions show two major populations, around 50% or 100% for the single-nucleotide polymorphisms (red, present in dbSNP), consistent with heterozygous or homozygous constitutional polymorphisms. The non-dbSNP variants (blue) occur mostly around 50%, likely indicative of 'personal single-nucleotide polymorphisms' (eg, variants not present in dbSNP). However, a number of the non-single-nucleotide polymorphism variants show substantial deviation from the expected 50 or 100% allelic fractions, indicative of true somatic variants or variants in regions of copy number variation. Merkel cell polyomavirus-positive cases: (**a**) Case 24, (**b**) Case 06, (**c**) Case 27, (**d**) Case 39, and (**e**) Case 18. Polyomavirus-negative cases: (**f**) Case 33, (**g**) Case 29, and (**h**) Case 21.

variants, those not present in the dbSNP showed skewing of the allele fractions indicating the presence of true somatically acquired variants, present at variable allele fractions due to stromal cell dilution, copy number variation, tumor heterogeneity, and so on (Figure 5). *RB1* variant allele fractions in the three cases (21, 29, and 33) with truncating retinoblastoma protein mutations ranged from 76.8 to 92.8%, with a mean of 85.2% (Figure 6). The increased allele fractions of *RB1* truncating mutations to greater than 50% likely represent a homozygous mutation within tumor cells, which are diluted in a background of non-tumor cells. However, it is not possible to determine whether the *RB1* mutations in each tumor represent a homozygous variant in a heterozygous background *vs* a homozygous acquired mutation. The number of genes with single-nucleotide variations occurring at an allele frequency ±5% within that of *RB1*, showed high variability between cases (Supplementary Table 1). This set included 10 genes for case 21, 31 genes for case 31, and 210 genes for case 29. None of the genes with single-nucleotide variations clustering around *RB1* were recurrent among all three cases.

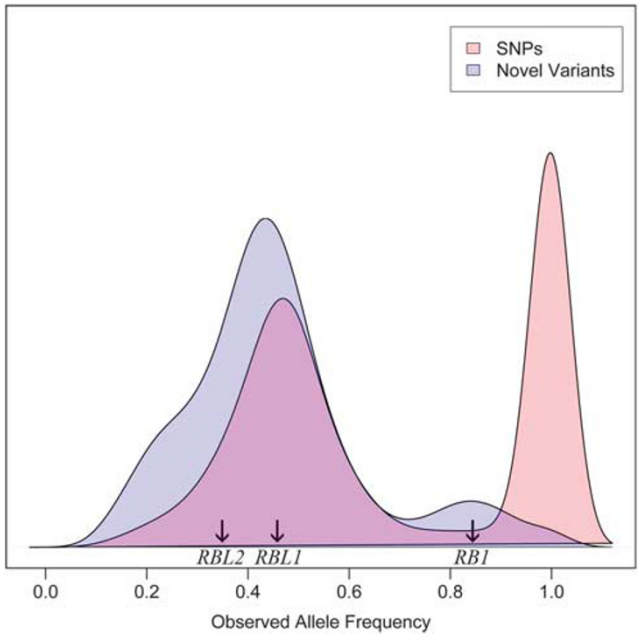

Figure 6 Combined allele frequency for all Merkel cell carcinoma cases. The frequency of retinoblastoma gene (*RB1*) non-single-nucleotide polymorphisms occurs around 85%. Other retinoblastoma pathway genes occur at lower allelic frequencies, including *RBL1* (around 45%) and *RBL2* (around 35%).

Table 6 Variants discovered in Merkel cell carcinoma cases that are also found in the Catalog of somatic mutations in cancer (COSMIC) database

24		*06*		*27*		*39*		*18*		*33*		*29*		*21*	
Gene	*Amino acid*	*Gene*	*Amino acid*	*Gene*	*Amino acid*	*Gene*	*Amino acid*	*Gene*	*Amino acid*	*Gene*	*Amino acid*	*Gene*	*Amino acid*	*Gene*	*Amino acid*
[a]ARMC4	D425Y	[a]AGBL5	V695I	ATP13A3	G1024S	[a]ARMC4	D425Y	[a]ARMC4	D425Y	ADAMTS19	L533F	ACAD10	P55H	ABHD5	R114L
BCL9	S1213L	C14orf93	R376H	BSN	P1482L	AZI1	P418L	ATP10B	R1023Q	ADCY10	E939K	ADAMTS18	P1186S	ACSL5	P587L
BTBD19	T76S	[a]GLUD2	G35R	C1orf125	A868T	C16orf72	R122Q	C12orf10	R188[b]	[a]AGBL5	V695I	ARID1A	R1721[b]	ATP11B	E362K
COL15A1	R772W	IVL	V420G	CCDC80	A559S	CYHR1	W141S	C12orf10	R188Q	ARHGEF12	S676F	B4GALNT4	F426Y	CCDC54	S320F
[a]FOXK1	T683P	PDGFB	R224W	EPN3	R170H	DRD4	Q287P	C9orf85	K29[b]	CDH20	R140Q	C6orf221	G155R	CCNJL	V151I
[a]LYZL2	A29G	ZFAT	A594T	FGD2	V127G	FBXO11	I780V	COL4A4	R50I	CDH9	R678S	CADPS	E287K	CDKN2A	P69S
NEDD4	E94K	[a]ZNRF4	S14T	[a]FOXK1	T683P	FRMPD2	Q798R	CYP4V2	R232[b]	CPAMD8	V355I	CASZ1	T1096M	CPEB4	R493C
OR9Q1	H56Q			HSPBP1	G25V	KCNK6	R37Q	DNAH10	E1432K	DNAH6	E3236K	CATSPER1	A714V	CRYBG3	R572C
RANGAP1	V268G			LRP2	R3646H	[a]LYZL2	A29G	EGFR	G719A	FCAR	M61I	CCDC154	V21I	DISC1	S301F
SIGLEC10	R205S			[a]LYZL2	A29G	OR2M4	T267M	EPX	L72I	[a]FOXK1	T683P	CDC16	P562L	DNAH5	R2639Q
[a]SLC25A26	S41N			NF1	D176E	TBC1D16	T189M	FN3KRP	V223I	GABRQ	S286L	DCAF12L2	P334L	FNIP2	G539R
SMCR7L	D398Y			NUP88	I126T	TET2	Y867H	[a]FOXK1	T683P	LRRC32	E231Q	EPHA3	G633E	FRK	E188K
SPTBN4	V937I			[a]PLEC	T4429M	ZMYND10	R340Q	GCN1L1	L595F	ME1	E227K	FAT3	G618E	GALNT13	R194Q
				PRR12	Q772L			[a]GLUD2	G35R	MLLT6	A327T	FBRSL1	A293T	GBP3	Q136[b]
				SCGB1C1	E47D			GRM3	E538K	NNMT	E233K	FPR3	R315C	GNA14	E66K
				[a]SLC25A26	S41N			KCNA4	R598W	NTNG1	R336Q	GATA6	E579K	GPR132	R151Q
				TCIRG1	R28W			KCNAB1	W231[b]	NUCB1	R87[b]	GRASP	S387F	GUCY1A2	S712L
				TSHZ1	T112P			LMO2	Q126E	OR4K17	A108V	GRIN2A	D1035N	HSPG2	G3138R
								LPPR5	R246[b]	P2RY12	E188K	GRM1	A184T	HYDIN	E1542K
								MAP2	S312L	PIK3CA	E545K	HHIP	G64R	LILRA5	R218C
								MIER2	D351N	[a]PLEC	T4429M	KCNQ3	E656K	LIMK1	E375K
								MYO1G	R641C	PTPRO	E854K	KCNS2	E438K	LRBA	T1588M
								NLRP3	R920[b]	SIGLEC6	A251T	KIF3A	R206C	[a]LYZL2	A29G
								OR5V1	S313F	SLC24A5	E53K	KIF5A	S831F	MMP7	R127[b]
								PCSK1N	S4A	[a]SLC25A26	S41N	MAGEC3	C26Y	MYO18B	E2241K
								PER1	T866P	SOX5	D221N	MCOLN2	R217W	NOC2L	D699N
								PRKD1	D378N	STXBP5L	R789[b]	MN1	E1048K	[a]OR11G2	G49D
								PTPRS	P287L	[a]TP53	R196[b]	NDN	E257K	OR13C4	D191N
								SMARCA1	Q35E	ZCCHC4	D72H	NRXN1	G1406E	OR14J1	P280S
								TEK	R522C	ZNF717	V230A	NUCB2	R173H	OR6Y1	I118N
								TFPI2	R222C	[a]ZNRF4	S14T	NUP93	E182K	[a]PCLO	R3831C
								TLE6	R165Q			NWD1	E182K	POLB	G80R
								TRIM38	P438S			OR10K2	S310F	PRMT7	G206R
								ZNF717	V230A			[a]OR11G2	G49D	RAG2	R148Q
								[a]ZXDB	E122K			PCDHGA1	R293C	RB1	W195[b]
								[a]ZXDB	E123A			[a]PCLO	R1507K	SALL2	P719S
												PLCXD3	K169E	SAMD11	S171L
												POLE	P1601S	SCAF1	P22L
												PROKR2	R85C	SFMBT1	R195H
												PTF1A	R296[b]	SLC30A3	A111V
												RCOR2	R254Q	TBX18	H401Y
												RNF111	S206L	TBX21	R400[b]
												RRP7A	N65S	TGFBI	M502V
												RSPO1	W153[b]	[a]TP53	R156P
												RXFP3	S115F	[a]TP53	R342[b]
												RYR2	E4137K	[a]TTN	E25755K
												SEMA4D	V167I		

Table 6 (Continued)

24		06		27		39		18		33		29		21	
Gene	*Amino acid*	*Gene*	*Amino acid*	*Gene*	*Amino acid*	*Gene*	*Amino acid*	*Gene*	*Amino acid*	*Gene*	*Amino acid*	*Gene*	*Amino acid*	*Gene*	*Amino acid*
												SEMA5A	E751K		
												SI	D1193N		
												SLC22A25	R494Q		
												[a]SLC25A26	S41N		
												TLR4	R257C		
												TMPRSS11E	A389S		
												[a]TTN	E17393K		
												UGT1A10	F171Y		
												WDR62	R496Q		
												ZDBF2	S1730L		
												ZDHHC4	C151R		
												[a]ZXDB	E122K		
												[a]ZXDB	E123A		

[a]Indicates recurrently mutated genes.
[b]Stop codon.

Comparison with Published Data Sets

To investigate whether the genetic signature of Merkel cell carcinoma is unique or whether it shows similarity to other cancer types, we compared the gene variants found in Merkel cell carcinoma to publicly available cancer-associated genetic mutations in the Catalog of Somatic Mutations in Cancer (COSMIC) database (Table 6). On average, 28 variants per case were present in COSMIC, with a range from 7 to 61. Only 13 of these mutations represented recurrent mutations, occurring in at least two Merkel cell carcinoma cases. Recurrently mutated variants occurred in *AGBL2*, *ARMC4*, *FOXK1*, *LYZL2*, *SLC25A26*, *GLUD2*, *ZNRF4*, *PLEC*, *ZXDB*, *TP53*, *OR11G2*, *PCLO*, and *TTN*. The most frequently mutated genes present in COSMIC were *LYZL2*, *FOXK1*, and *SLC25A26*, with each having mutations in four of eight cases. Overall, it does not appear that the gene mutations found in Merkel cell carcinoma show compelling overlap with other well-studied cancer types, suggesting a unique pathogenesis in Merkel cell carcinoma.

Discussion

For the first time, whole exome sequencing was used as an unbiased tool to characterize the genetic landscape of Merkel cell carcinoma, utilizing archival formalin-fixed paraffin-embedded tissue. This is in contrast to previous studies that have taken targeted approaches to define somatic mutations in Merkel cell carcinoma. These genes include *PIK3CA*, *TP53*, and *PTEN*.[40–43] In our study cases, *PIK3CA* and *TP53*, but not *PTEN*, were found to harbor mutations, but only in small number of cases (Table 5). Using the gene level recurrence as a metric, we identified the retinoblastoma pathway as critical to Merkel cell carcinoma pathogenesis. We acknowledge, however, that without concurrent exome data from paired normal tissue in each case, we cannot fully exclude that the 'mutations' identified represent benign polymorphisms not present in dbSNP; estimates of such 'personal single-nucleotide variants' are $\sim$200 coding region variants per normal individual and are therefore unlikely to account for all variants identified in each case.[44] To further ameliorate this potential source of false discovery, we compared our data with the COSMIC database of known somatic mutations in cancer, looked only for recurrent mutations present in more than one case (and therefore unlikely to represent low prevalence polymorphisms), and examined the variant allele fraction of potential mutations.

Other groups have also provided evidence for retinoblastoma pathway dysregulation in subsets of Merkel cell carcinoma. Merkel cell polyomavirus has a large T antigen LXCXE domain that, when expressed, binds directly to retinoblastoma protein.[45] Several lines of evidence have suggested

that in polyomavirus-positive cases, retinoblastoma dysregulation occurs secondary to maintenance and expression of the large T antigen, and specifically the retinoblastoma protein-binding region of the large T antigen.[12,15–21] The large T antigen of integrated Merkel cell polyomavirus has been shown to have varying mutations among Merkel cell carcinoma cases, but the mutations invariably spare the retinoblastoma protein-binding domain.[18] At the human genome level, prior studies by others have provided evidence of loss of *RB1* in subsets of Merkel cell carcinoma. In 1997, Leonard and Hayward[46] demonstrated a loss of heterozygosity of 13q14, the chromosomal region of *RB1* locus, in 18/24 (75%) of Merkel cell carcinoma cases and additionally used western blot analysis to show that cell lines derived from 9/18 of these patients had an absence of detectable retinoblastoma protein. Later, array comparative genomic hybridization studies involving the *RB1* locus by Van Gele *et al*[47] and Paulson *et al*[48] showed the deletion of 13q in 8/24 (33%) Merkel cell carcinoma cases and 13q14-13q21 in 6/23 (26%) Merkel cell carcinoma cases, respectively.

We found that polyomavirus-negative cases with little or no detectable polyomavirus by sensitive real-time polymerase chain reaction had truncating, nonsense *RB1* mutations. Even though two of the five polyomavirus-positive cases showed *RB1* deletions (one case with a deletion and one with copy number variation), there were no single-nucleotide variation truncating nonsense mutations within polyomavirus-positive cases. This suggests a unique genetic mechanism to *RB1* inactivation occurring within polyomavirus-negative cases; however, given the small sample size in this study, we cannot exclude that such mutations may also be present in polyomavirus-positive cases. Further we note that,

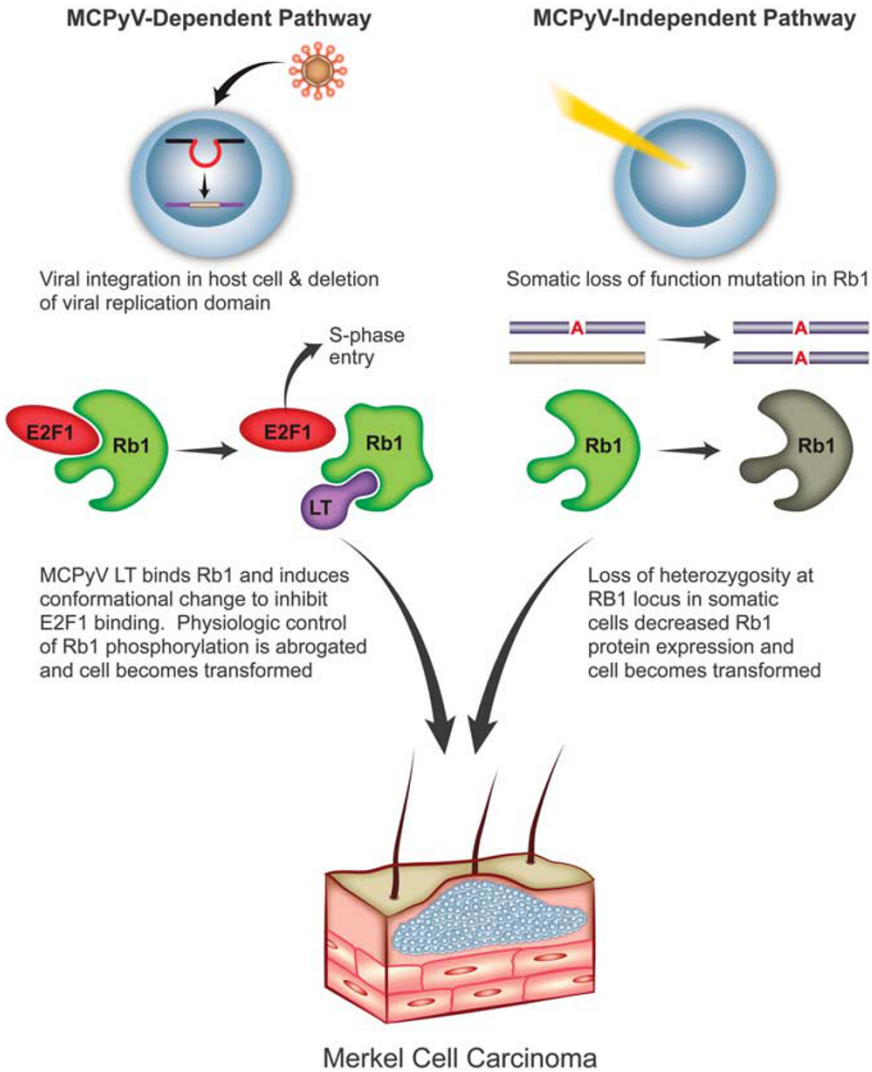

Figure 7 Proposed mechanism of Merkel cell carcinoma oncogenesis involving the retinoblastoma pathway. In this model, the retinoblastoma pathway is dysregulated in both Merkel cell polyomavirus (MCPyV)-positive and polyomavirus-negative cases, which leads to an indistinguishable morphological and clinical phenotype.

although two polyomavirus-negative cases had DNA-level mutations in *RB1*, one resulted in copy loss of *RB1*, and the other a 68 amino-acid deletion near the C-terminus, and may result in different functional effects than the *RB1* truncating mutations seen in polyomavirus-negative cases.

Other groups have reported a similar correlation between retinoblastoma protein expression and Merkel cell polyomavirus copy number. Bhatia *et al*[22] linked the presence of retinoblastoma protein by immunohistochemistry to cases of Merkel cell carcinoma with a polyomavirus load of at least 0.06 viral copies/cell ($n=9$), as detected by real-time polymerase chain reaction. Merkel cell carcinoma cases with polyomavirus viral loads ranging from 0 to 0.0035 viral copies/cell ($n=14$) had an absence of retinoblastoma protein. However, a study by Houben *et al*[49] showed retinoblastoma protein expression by immunohistochemistry in every tested Merkel cell carcinoma case ($n=50$), including those with extremely low levels of viral copies/cell. It is possible that the discrepant findings were due to differing antibodies used or antigen retrieval techniques. A recent gene expression study by Harms *et al*[50] comparing transcripts between Merkel cell polyomavirus-positive and polyomavirus-negative Merkel cell carcinoma cases showed that virus-negative cases have a relative 2.4-fold lower expression of *RB1* and that retinoblastoma protein immunohistochemistry corresponded to Merkel cell polyomavirus status and *RB1* transcript levels. In this study, we link the presence of decreased retinoblastoma protein expression to specific genetic mutations. Overall, these mutations tend to occur in Merkel cell carcinoma cases with low to no detectable polyomavirus arguing that retinoblastoma abrogation is required for Merkel cell carcinoma pathogenesis in the absence of polyomavirus.

Using an unbiased genomic approach, we identified the retinoblastoma pathway as critical in Merkel cell carcinoma pathogenesis and validated that retinoblastoma protein was decreased or absent in Merkel cell carcinoma cases with *RB1* mutations. Further, we demonstrate that in Merkel cell carcinoma cases with intact retinoblastoma protein expression and without the evidence of *RB1* mutations, the majority of retinoblastoma protein exists in the active, unphosphorylated form, despite frequent tumor cell division. This finding suggests retinoblastoma protein dysregulation by an alternative pathway in some cases of polyomavirus-positive Merkel cell carcinoma, such as direct large T antigen binding and subsequent non-phosphorylation-dependent inactivation of retinoblastoma protein. On the basis of these findings, we propose a model of Merkel cell carcinoma oncogenesis by which two separate pathways, a polyomavirus-dependent pathway in which retinoblastoma protein is functionally inactivated and a polyomavirus-independent pathway in which *RB1* sustains somatic mutation, both of which require retinoblastoma protein dysregulation to produce an overlapping Merkel cell carcinoma phenotype (Figure 7). An alternative explanation for *RB1* mutation in Merkel cell carcinoma might include the proposed model of hit-and-run oncogenesis in which Merkel cell polyomavirus integrates in to the host genome of all Merkel cell carcinoma cases, does genetic damage, either persists as clonally integrated virus or is expelled from the human genome by various repair mechanisms.[51] Integrating our data with this model, Merkel cell polyomavirus may initiate Merkel cell carcinoma tumorogenesis in a subset of cases, including a genetic 'hit' to *RB1* such as nonsense truncating mutations. After this 'hit' occurs, Merkel cell polyomavirus is no longer necessary for Merkel cell carcinoma progression and maintenance and the virus leaves ('runs' from) the human host genome. In any case, the retinoblastoma pathway appears to have an important role in Merkel cell carcinoma. Therapeutic targeting of the retinoblastoma pathway, specifically downstream of the retinoblastoma protein itself, by small-molecule inhibitors has been proposed in several tumor types with retinoblastoma protein loss (recently reviewed[52]). Perhaps future research focused on targeting the retinoblastoma pathway in Merkel cell carcinoma may offer clinical benefit for this highly aggressive cancer.

Acknowledgments

We thank Xiaopei Zhu for assistance with DNA extraction. We also thank the Genome Technology Access Center in the Department of Genetics at Washington University School of Medicine for assistance with DNA sequencing.

Disclosure/conflict of interest

The authors declare no conflict of interest.

References

1 Calder KB, Smoller BR. New insights into merkel cell carcinoma. Adv Anat Pathol 2010;17:155–161.
2 Agelli M, Clegg LX, Becker JC, *et al.* The etiology and epidemiology of merkel cell carcinoma. Curr Probl Cancer 2010;34:14–37.
3 Albores-Saavedra J, Batich K, Chable-Montero F, *et al.* Merkel cell carcinoma demographics, morphology, and survival based on 3870 cases: a population based study. J Cutan Pathol 2010;37:20–27.
4 Lemos BD, Storer BE, Iyer JG, *et al.* Pathologic nodal evaluation improves prognostic accuracy in Merkel cell carcinoma: analysis of 5823 cases as the basis of the first consensus staging system. J Am Acad Dermatol 2010;63:751–761.
5 Duncavage EJ, Zehnbauer BA, Pfeifer JD. Prevalence of Merkel cell polyomavirus in Merkel cell carcinoma. Mod Pathol 2009;22:516–521.

6 Feng H, Shuda M, Chang Y, *et al.* Clonal integration of a polyomavirus in human Merkel cell carcinoma. Science 2008;319:1096–1100.
7 Sihto H, Kukko H, Koljonen V, *et al.* Clinical factors associated with Merkel cell polyomavirus infection in Merkel cell carcinoma. J Natl Cancer Inst 2009;101:938–945.
8 Chen T, Hedman L, Mattila PS, *et al.* Serological evidence of Merkel cell polyomavirus primary infections in childhood. J Clin Virol 2011;50:125–129.
9 Pastrana DV, Tolstov YL, Becker JC, *et al.* Quantitation of human seroresponsiveness to Merkel cell polyomavirus. PLoS Pathog 2009;5:e1000578.
10 Tolstov YL, Pastrana DV, Feng H, *et al.* Human Merkel cell polyomavirus infection II. MCV is a common human infection that can be detected by conformational capsid epitope immunoassays. Int J Cancer 2009;125:1250–1256.
11 Dalianis T, Hirsch HH. Human polyomaviruses in disease and cancer. Virology 2013;437:63–72.
12 Chang Y, Moore PS. Merkel cell carcinoma: a virus-induced human cancer. Annu Rev Pathol 2012;7:123–144.
13 Duncavage EJ, Magrini V, Becker N, *et al.* Hybrid capture and next-generation sequencing identify viral integration sites from formalin-fixed, paraffin-embedded tissue. J Mol Diagn 2011;13:325–333.
14 Martel-Jantin C, Filippone C, Cassar O, *et al.* Genetic variability and integration of Merkel cell polyomavirus in Merkel cell carcinoma. Virology 2012; 426:134–142.
15 Angermeyer S, Hesbacher S, Becker JC, *et al.* Merkel cell polyomavirus positive Merkel cell carcinoma cells do not require expression of the viral small T antigen. J Invest Dermatol 2013;133:2059–2064.
16 Cheng J, Rozenblatt-Rosen O, Paulson KG, *et al.* Merkel cell polyomavirus large t antigen has growth promoting and inhibitory activities. J Virol 2013;87: 6116–6126.
17 Demetriou SK, Ona-Vu K, Sullivan EM, *et al.* Defective DNA repair and cell cycle arrest in cells expressing Merkel cell polyomavirus T antigen. Int J Cancer 2012; 131:1818–1827.
18 Houben R, Adam C, Baeurle A, *et al.* An intact retinoblastoma protein-binding site in Merkel cell polyomavirus large T antigen is required for promoting growth of Merkel cell carcinoma cells. Int J Cancer 2012;130:847–856.
19 Houben R, Shuda M, Weinkam R, *et al.* Merkel cell polyomavirus-infected Merkel cell carcinoma cells require expression of viral T antigens. J Virol 2010;84: 7064–7072.
20 Sastre-Garau X, Peter M, Avril MF, *et al.* Merkel cell carcinoma of the skin: pathological and molecular evidence for a causative role of MCV in oncogenesis. J Pathol 2009;218:48–56.
21 Sihto H, Kukko H, Koljonen V, *et al.* Merkel cell polyomavirus infection, large T antigen, retinoblastoma protein and outcome in Merkel cell carcinoma. Clin Cancer Res 2011;17:4806–4813.
22 Bhatia K, Goedert JJ, Modali R, *et al.* Merkel cell carcinoma subgroups by Merkel cell polyomavirus DNA relative abundance and oncogene expression. Int J Cancer 2010;126:2240–2246.
23 Handschel J, Muller D, Depprich RA, *et al.* The new polyomavirus (MCPyV) does not affect the clinical course in MCCs. Int J Oral Maxillofac Surg 2010;39: 1086–1090.
24 Schrama D, Peitsch WK, Zapatka M, *et al.* Merkel cell polyomavirus status is not associated with clinical course of Merkel cell carcinoma. J Invest Dermatol 2011;131:1631–1638.
25 Asioli S, Righi A, de Biase D, *et al.* Expression of p63 is the sole independent marker of aggressiveness in localised (stage I-II) Merkel cell carcinomas. Mod Pathol 2011;24:1451–1461.
26 Kuwamoto S, Higaki H, Kanai K, *et al.* Association of Merkel cell polyomavirus infection with morphologic differences in Merkel cell carcinoma. Hum Pathol 2011;42:632–640.
27 Teman CJ, Tripp SR, Perkins SL, *et al.* Merkel cell polyomavirus (MCPyV) in chronic lymphocytic leukemia/small lymphocytic lymphoma. Leuk Res 2011;35: 689–692.
28 Cimino PJ Jr., Bahler DW, Duncavage EJ. Detection of Merkel cell polyomavirus in chronic lymphocytic leukemia T-cells. Exp Mol Pathol 2013;94:40–44.
29 DePristo MA, Banks E, Poplin R, *et al.* A framework for variation discovery and genotyping using next-generation DNA sequencing data. Nat Genet 2011;43: 491–498.
30 McKenna A, Hanna M, Banks E, *et al.* The Genome Analysis Toolkit: a MapReduce framework for analyzing next-generation DNA sequencing data. Genome Res 2010;20:1297–1303.
31 Li H, Handsaker B, Wysoker A, *et al.* The Sequence alignment/Map format and SAMtools. Bioinformatics 2009;25:2078–2079.
32 Ye K, Schulz MH, Long Q, *et al.* Pindel: a pattern growth approach to detect break points of large deletions and medium sized insertions from paired-end short reads. Bioinformatics 2009;25:2865–2871.
33 Chen K, Wallis JW, McLellan MD, *et al.* BreakDancer: an algorithm for high-resolution mapping of genomic structural variation. Nat Methods 2009;6:677–681.
34 Li J, Lupat R, Amarasinghe KC, *et al.* CONTRA: copy number analysis for targeted resequencing. Bioinformatics 2012;28:1307–1313.
35 Bamford S, Dawson E, Forbes S, *et al.* The COSMIC (Catalogue of Somatic Mutations in Cancer) database and website. Br J Cancer 2004;91:355–358.
36 Forbes SA, Bindal N, Bamford S, *et al.* COSMIC: mining complete cancer genomes in the Catalogue of Somatic Mutations in Cancer. Nucleic Acids Res 2011;39:D945–D950.
37 Walter MJ, Shen D, Ding L, *et al.* Clonal architecture of secondary acute myeloid leukemia. N Engl J Med 2012;366:1090–1098.
38 Higaki-Mori H, Kuwamoto S, Iwasaki T, *et al.* Association of Merkel cell polyomavirus infection with clinicopathological differences in Merkel cell carcinoma. Hum Pathol 2012;43:2282–2291.
39 Adzhubei IA, Schmidt S, Peshkin L, *et al.* A method and server for predicting damaging missense mutations. Nat Methods 2010;7:248–249.
40 Hafner C, Houben R, Baeurle A, *et al.* Activation of the PI3K/AKT pathway in Merkel cell carcinoma. PLoS One 2012;7:e31255.
41 Lassacher A, Heitzer E, Kerl H, *et al.* p14ARF hypermethylation is common but INK4a-ARF locus or p53 mutations are rare in Merkel cell carcinoma. J Invest Dermatol 2008;128:1788–1796.
42 Nardi V, Song Y, Santamaria-Barria JA, *et al.* Activation of PI3K signaling in Merkel cell carcinoma. Clin Cancer Res 2012;18:1227–1236.

43 Van Gele M, Leonard JH, Van Roy N, *et al.* Frequent allelic loss at 10q23 but low incidence of PTEN mutations in Merkel cell carcinoma. Int J Cancer 2001;92:409–413.
44 Bamshad MJ, Ng SB, Bigham AW, *et al.* Exome sequencing as a tool for Mendelian disease gene discovery. Nat Rev Genet 2011;12:745–755.
45 Shuda M, Feng H, Kwun HJ, *et al.* T antigen mutations are a human tumor-specific signature for Merkel cell polyomavirus. Proc Natl Acad Sci USA 2008;105: 16272–16277.
46 Leonard JH, Hayard N. Loss of heterozygosity of chromosome 13 in Merkel cell carcinoma. Genes Chromosomes Cancer 1997;20:93–97.
47 Van Gele M, Speleman F, Vandesompele J, *et al.* Characteristic pattern of chromosomal gains and losses in Merkel cell carcinoma detected by comparative genomic hybridization. Cancer Res 1998;58: 1503–1508.
48 Paulson KG, Lemos BD, Feng B, *et al.* Array-CGH reveals recurrent genomic changes in Merkel cell carcinoma including amplification of L-Myc. J Invest Dermatol 2009;129:1547–1555.
49 Houben R, Schrama D, Alb M, *et al.* Comparable expression and phosphorylation of the retinoblastoma protein in Merkel cell polyoma virus-positive and negative Merkel cell carcinoma. Int J Cancer 2010;126: 796–798.
50 Harms PW, Patel RM, Verhaegen ME, *et al.* Distinct gene expression profiles of viral- and nonviral-associated merkel cell carcinoma revealed by transcriptome analysis. J Invest Dermatol 2013;133:936–945.
51 Houben R, Grimm J, Willmes C, *et al.* Merkel cell carcinoma and Merkel cell polyomavirus: evidence for hit-and-run oncogenesis. J Invest Dermatol 2012;132: 254–256.
52 Clem BF, Chesney J. Molecular pathways: regulation of metabolism by RB. Clin Cancer Res 2012;18:6096–6100.

Supplementary Information accompanies the paper on Modern Pathology website (http://www.nature.com/modpathol)